

Research on the Stability of Vehicle Active Shock Absorber Based on Intelligent Control System

Mingjie Li*

Liaoning mechatronics college, Dandong 118009, China

*Corresponding author e-mail:limingjie@lnmec.net.cn

Abstract. The traditional vehicle suspension vibration reduction design method uses a fixed damping coefficient to reduce the vibration of the elastic element, and does not consider the different vibration intensity caused by different road conditions and vehicle speeds, and the vibration reduction effect is poor. A finite element design method for vehicle suspension shock absorption optimization is proposed to analyse the function and structure of vehicle suspension shock absorbers. We use the first-order optimization method in the ANSYS finite element software to carry out the optimal design of vehicle suspension damping, and take the damping force of the suspension shock absorber as the optimization objective to carry out the finite element optimization design of the vehicle suspension damping. This ensures that the vibration of the vehicle body is rapidly attenuated, so that the body can quickly reach a stable state. The results show that the fuzzy control strategy can greatly suppress the acceleration of the vehicle body and the dynamic load of the tire, reduce the dynamic travel of the suspension, and the ride comfort, driving safety and operation stability of the vehicle have been significantly improved, and the system suspension has a good comprehensive performance.

Keywords: Semi-active suspension, fuzzy control strategy, magnetorheological shock absorber current, three-dimensional structure.

1. Introduction

During the driving process of the car, due to the excitation of the road surface, the body will vibrate, which affects the ride comfort of the car. Traditional car suspensions use passive suspensions to damp vibrations from the road surface. However, the parameters of the passive suspension are designed by comprehensively considering typical working conditions, which is a compromise between various working conditions. Once set, they are fixed, so it is difficult to adapt to complex and changeable road conditions [1]. Active suspension can provide an additional power source to resist the vibration of the vehicle body, and the study of its control algorithm is one of the hotspots in vehicle ride comfort research. The predecessors have done a lot of work in the research of vehicle suspension vibration reduction control algorithm: some scholars use the optimal control method to reduce the vibration of the suspension, because it is difficult to determine the optimal weighting coefficient, and it is difficult to implement. Some scholars use the Backstepping method to control the distribution of the system, but the problem is the surge in the amount of calculation. The fuzzy control algorithm is simple, does not require an accurate mathematical model of the system, and has good adaptability, which is a powerful tool to solve the suspension vibration control.

In this paper, a vibration model of the active suspension of the whole vehicle is established, and the fuzzy control is used to reduce the vibration of the vehicle suspension [2]. The vibration effect of the suspension using the fuzzy control is compared with that of the passive suspension, and it is verified that the active suspension using the fuzzy control theory can reduce the vibration of the vehicle. Vibration feasibility.

2. Design Process

2.1 Design of the inner loop controller

The output signal u of the inner loop controller is used as the input signal of the actuator to control the actuator to generate the required control force [3]. The expression of u is:

$$u = \frac{v}{\gamma \Lambda \sqrt{P_s - \text{sgn}(v) \frac{\text{sat}_{F1}(F)}{\Lambda}}} \quad (1)$$

V is derived from the following two equations:

$$\begin{cases} \dot{Z}_c = -\lambda_c Z_c - K_c \lambda_c (F - \text{sat}_{F1}(F)) \\ v = \alpha \Lambda^2 Z_2 + (\beta - \lambda_t) \text{sat}_{F1}(F) + \lambda_t (F_{cmd} + Z_c) + \dot{F}_{cmd} + \dot{Z}_c \end{cases} \quad (2)$$

In the above control system, select $\lambda_t = 1260$, $\lambda_c = 2000$, $K_c = 10$.

2.2 Design of the outer loop controller

The outer loop controller is a parallel distribution compensator (PDC) based on TS type fuzzy inference system. Taking the road disturbance input r and the control signal F_{cmd} as input, the TS model can be linearized into a linear system [4]. The parallel distribution compensator PDC includes every control rule designed by TS type fuzzy controller linear interpolation.

2.2.1 T-S fuzzy inference system. T

The input r and F_{cmd} of the inner loop control system are roughly linear, and F_{cmd} is used to replace F in the system dynamics equation to obtain:

$$z_l = Az_l + B_1 r + B_2 F_{cmd} \quad (3)$$

The following is a description of linear equations using TS fuzzy inference system to achieve nonlinear control requirements. For small disturbances, the control performance is measured by the vertical vibration acceleration of the body, and for larger disturbances, the control performance is measured by the suspension travel. It is suitable to use the TS type fuzzy inference system: first, it can obtain different control rules according to the different amplitudes of the input disturbance on the road surface; secondly, it can provide an optimized control structure for the current target [5]. The amplitude of the suspension stroke is used to adjust the vertical vibration acceleration of the body. The description of the TS model is based on the variable, the amplitude h of the suspension dynamic stroke. The amplitude h of the suspension dynamic stroke is defined as:

$$\{h, U, (T_h^1, \dots, T_h^m), (\mu_h^1, \dots, \mu_h^m)\} \quad (4)$$

In the formula, $U = [0, \bar{z}_1]$ is the value range of h , T_h^i is the parameter name of h , and μ_h^i is the membership function corresponding to T_h^i . The control rules of the TS model have the following form:

$$\text{Rule } i: \text{IF } h \text{ is } T_h^i, \text{ THEN } \dot{z}_l = Az_l + B_1 r + B_2 F_{cmd}, i=1, 2, \dots, m \quad (5)$$

The membership function is described by a piecewise polynomial piecewise combination, and the highest order of the polynomial is 7. The coordinate values of each membership function are parameterized. The first setting parameter T_h^1 , μ_h^1 of the membership function is given by:

$$\mu_h^1 = \begin{cases} 1 & \text{if } 0 \leq h \leq c_1 \\ 1 - P_{c_1, d_1}(h) & \text{if } c_1 \leq h \leq d_1 \\ 0 & \text{if } d_1 \leq h \end{cases} \quad (6)$$

Where $P_{c_i, d_i}(h)$ is a polynomial of degree 7. For the parameter T_h^i of the membership function, $i=2, (m-1)$, μ_h^i is given by,

$$\mu_h^i = \begin{cases} 0 & \text{if } 0 \leq h \leq a_i \\ P_{a_i, b_i}(h) & \text{if } a_i \leq h \leq b_i \\ 1 & \text{if } b_i \leq h \leq c_i \\ 1 - P_{c_i, d_i}(h) & \text{if } c_i \leq h \leq d_i \\ 0 & \text{if } d_i \leq h \leq \bar{z}_1 \end{cases} \quad (7)$$

For the last parameter T_h^m of the membership function, μ_h^m is given by,

$$\mu_h^m = \begin{cases} 0 & \text{if } 0 \leq h \leq a_m \\ P_{a_m, b_m}(h) & \text{if } a_m \leq h \leq b_m \\ 1 & \text{if } b_r \leq h \leq \bar{z}_1 \end{cases} \quad (8)$$

The subscripts of the above parameters are limited as follows: $a_i = c_{i-1}$, $b_i = d_{i-1}$, $i=2,3, m$. The coordinates of the membership function of the TS model, denoted by a_i , c_i , b_i , d_i are the carrier of the membership function parameter Pm: $P_m = [a_2 \cdots a_m \quad b_2 \cdots b_m \quad c_1 \cdots c_{m-1} \quad d_1 \cdots d_{m-1}]$.

2.2.2 TS inference model.

Finally, the nonlinear control requirements given by the linear dynamic equation (9) can be realized by TS fuzzy inference, and the fuzzy output is: $e(t) = C(t)z(t) + D(t)F_{cmd}(t)$

In the formula: $C(t) = \sum_{i=1}^m \eta_i(t)C_i$, $D(t) = \sum_{i=1}^m \eta_i(t)D_i$, and $\eta_i(t) = \frac{\mu_h^i(h(t))}{\sum_{j=1}^m \mu_h^j(h(t))}$, $i=1, 2, m$

The output e is represented by the λ_i and ρ_i parameters, which constitute the output vector Pp, $i=1, 2, m$. $P_p = [\lambda_1 \cdots \lambda_m \quad \rho_1 \cdots \rho_m]$. In this way, with the vectors Pm and Pp, the TS fuzzy inference system is constructed.

2.2.3 Parallel distribution of compensators

In this paper, a parallel distribution compensator is used to control the TS model. For each control rule, a static state feedback controller is designed and fuzzified. The key point is to use the same fuzzy set as the TS model to achieve fuzzification. In order to describe the problem more accurately, the control signal Fcmd can be expressed as:

$$F_{cmd}(t) = K(t)z(t) = \left(\sum_{i=1}^m \eta_i(t)K_i \right) z(t) \quad (9)$$

Since the output is represented by the vector Pp and the membership function is described by Pm, the parallel distribution compensator PDC is still described by the relevant parameters of Pp and Pm.

2.2.4 Parameter optimization based on genetic algorithm

As mentioned earlier, the parallel distribution compensator PDC can be expressed by the vectors Pm and Pp. Based on our existing empirical knowledge, it is difficult to select the optimal parameters of the vectors Pm and Pp to achieve a very good control effect. In order to achieve a better control

effect, we cannot only rely on our existing empirical knowledge for parameter selection. Here, we employ a genetic algorithm to select the optimal parameter values for the vectors Pm and Pp. The main operations of the standard genetic algorithm include: initializing the population, replication, crossover and mutation, and according to the control objective, the fitness function achieves the maximum value [6]. The fitness function used in this paper is:

$$J(P_m, P_p) = \frac{1}{J_1 + J_2 + J_3} \tag{10}$$

In:

$$J_1 = \begin{cases} 1500 \bar{x}_b^{(5)} & \text{if } \bar{x}_b^{(5)} < \frac{1}{3} \\ 1500(3 \bar{x}_b^{(5)})^4 & \text{if } \bar{x}_b^{(5)} \geq \frac{1}{3} \end{cases}$$

$$J_2 = \begin{cases} 0 & \text{if } \bar{x}_b^{(11)} \leq \frac{3}{2} \\ 100\left(\frac{2}{3} \bar{x}_b^{(11)} - 1\right) & \text{if } \bar{x}_b^{(11)} \geq \frac{3}{2} \end{cases} \tag{11}$$

$$J_3 = \begin{cases} 10^6 & \text{if } \bar{z}_1 - Z_1 < 10^{-4} \bar{z}_1 \\ 0 & \text{if } \bar{z}_1 - Z_1 > 10^{-4} \bar{z}_1 \end{cases}$$

Z1 is the peak value of the suspension dynamic travel under the action of road excitation with a peak value of 11cm. The control effect of the controller will be evaluated by computer simulation.

3. System Simulation

The parameters of the controller are listed in Table 1, and the corresponding membership function is shown in Figure 1 (the picture is quoted in A survey: fuzzily parameters and membership function in electrical applications).

Table 1. Relevant values of the parameter Pm of the C4fs membership function of the controller

a1	b1	c1	d1	a2	b2	c2	d2
—	—	1.4864	3.0646	1.4864	3.0646	5.0585	6.5626
a3	b3	c3	d3	a4	b4	c4	d4
5.0585	6.8183	7.3383	7.6669	7.3383	7.6669	—	—

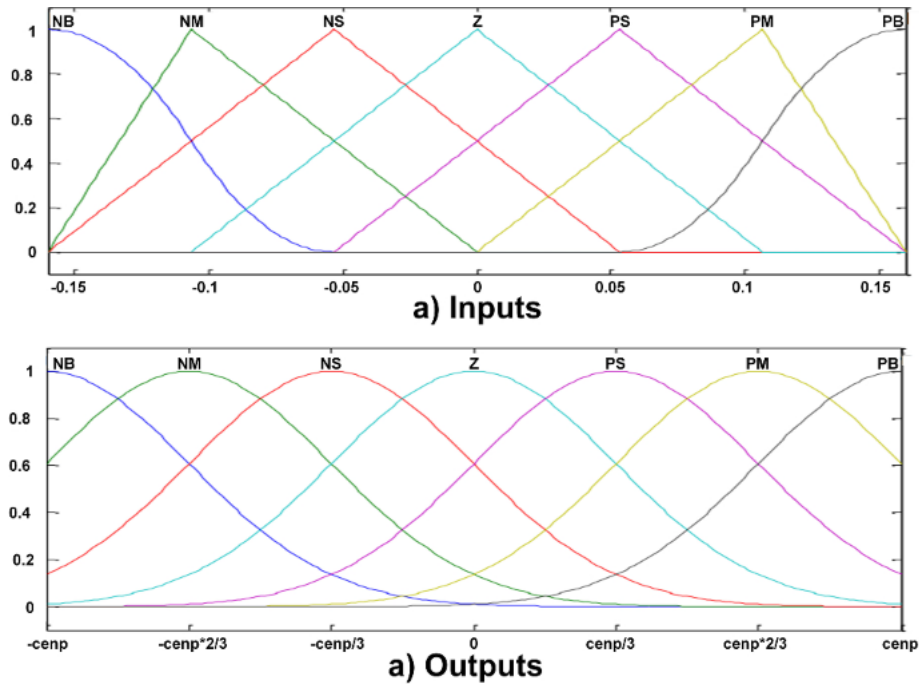


Figure 1. Membership functions of fuzzy controllers C2fs, C3fs and C4fs

Figure 2 shows the four performance indicators used to evaluate the performance of the controller versus time (the picture is quoted from A Real-Time Accurate Model and Its Predictive Fuzzy PID Controller for Pumped Storage Unit via Error Compensation). The solid line is the curve under closed-loop control, and the dashed line is the curve under no control [7]. These curves are given according to two cases where the road disturbance input peak is 5cm and 11cm respectively.

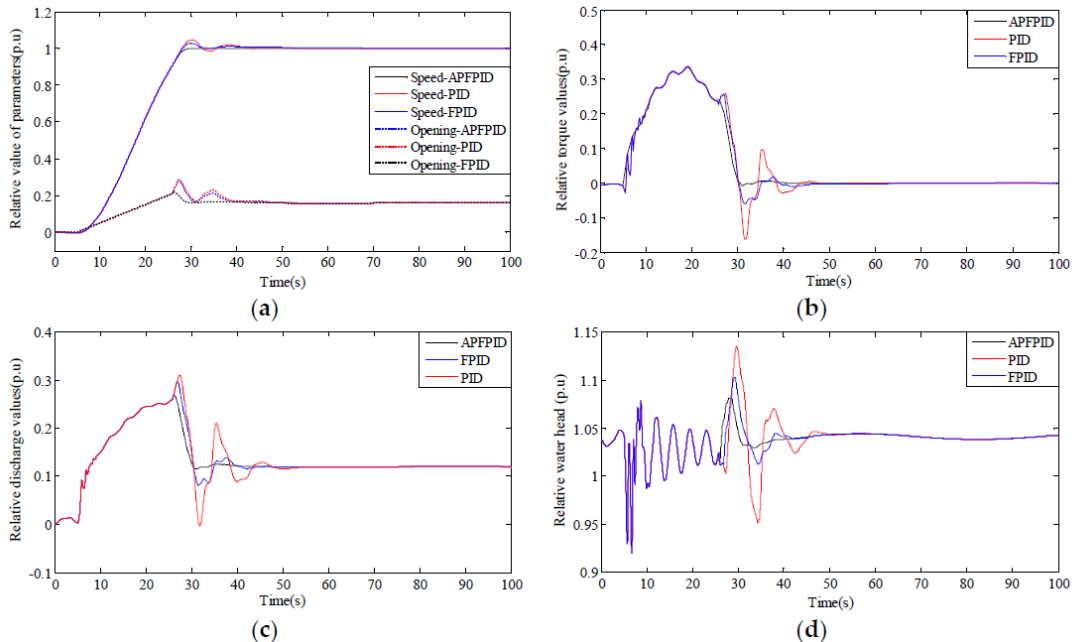


Figure 2. Three performance index curves of controller performance

In the wheel resonance frequency between 8 and 9 Hz, the electric wheel passive vibration damping system is significantly smaller than the traditional electric wheel vibration damping system in terms of the impact force on the motor, which verifies that the vibration isolation device plays a good role in improving the motor vibration. Compared with the passive vibration reduction system, the active vibration reduction system of the electric wheel has obvious advantages, which greatly

reduces the impact force on the motor, improves the working environment of the motor, and prolongs the working life of the motor to a certain extent [8]. All performance indicators have been significantly improved. Compared with the traditional electric wheel system, the passive vibration reduction system of the electric wheel has a significant reduction in the performance evaluation index, and the active vibration reduction system of the electric wheel further improves the ride comfort of the vehicle. Compared with the traditional electric wheel system, the electric wheel active vibration reduction system has obvious optimization in the performance index root mean square value. The two main optimization goals of body acceleration and motor impact force are reduced by 51.5% and 59.4% respectively. The relative dynamic load and suspension dynamic deflection are reduced by 41.8% and 33.3% respectively, which greatly improves the ride comfort and safety of the vehicle, and the reduction of the motor impact force improves the work of the drive motor. environment, thereby extending the life of the motor.

4. Conclusion

Based on the establishment of a nonlinear model of the vehicle with active suspension, the differential geometry theory is used to decouple the vehicle suspension system and conduct vibration reduction control. After the system is decoupled, the vertical motion, roll motion and roll motion of the suspension sprung mass are independent of each other, becoming an independent linear second-order system, and the motion of the system sprung mass is decoupled. The simulation results show that the vertical displacement, pitch angle and roll angle of the vehicle sprung mass vibration are greatly attenuated; the acceleration in each direction and the dynamic deflection at each wheel are also reduced to a certain extent, indicating that the decoupling vibration reduction control algorithm is effective.

Acknowledgements

Foundation of Liaoning Mechatronics College in 2021, the structural design of double— piston Hydraulic Limiting shock (No. ky202103)

References

- [1] Li Xu, Liu Bing, Chen Ying, et al. Research on shock absorption and anti-sway of chimney suspension inner cylinder-rotating friction damper. *Earthquake Engineering and Engineering Vibration*, 41(4) (2021) 12-18.
- [2] Mu Zengguo, Zhang Jiping, Li Hongming. The effect of prestress on the natural frequency of automobile shock absorbers. *Machinery Manufacturing and Automation*, 50(1) (2021) 44-48.
- [3] Feng Fan. Modeling and Simulation Analysis of Automobile Damping System Based on Finite Element Method. *Electronic Design Engineering*, 29(6) (2021) 45-50.
- [4] Ji Wenchao, Guo Shiru, Zhao Jing, et al. Simulation of quality testing methods for shock absorber lining kits in automotive chassis. *Computer Simulation*, 38(8) (2021) 58-66.
- [5] Gong Jun, Zhi Xudong, Fan Feng. Influence of dynamic coupling of suspension system on seismic response and ultimate bearing capacity of 1000kV outgoing frame. *Chinese Journal of Civil Engineering*, 55(1) (2022) 111-119.
- [6] Liu Jianjun, Sun Yixia, Li Sheng. Multi-objective optimization of vehicle suspension system under time-delay positive feedback control. *Computer Applications and Software*, 38(4) (2021) 65-69.
- [7] Xing Xianqiang, Cao Wenquan, Wang Cunyu. Ribbon structure of 55SiCr spring steel wire for automotive suspension system. *Iron and Steel*, 55(3) (2020) 67-75.
- [8] Liu Jianjun, Sun Yixia, Li Sheng. Time-delay feedback control and parameter optimization of automotive suspension system. *Mechatronic Engineering*, 37(1) (2020) 54-60.